

## Search for Cosmic-Ray Antimatter

G. F. Smoot, A. Buffington, and C. D. Orth

*Space Sciences Laboratory and Lawrence Berkeley Laboratory, University of California, Berkeley, California 94720*

(Received 21 April 1975)

In a sample of  $1.5 \times 10^4$  helium and  $4.0 \times 10^4$  higher-charged nuclei, obtained with balloon-borne superconducting magnetic spectrometers, we find the ratio of antinuclei to nuclei in the cosmic rays to be less than  $8 \times 10^{-5}$  for rigidities (momentum/charge) between 4 and 33 GV/c and less than  $10^{-2}$  between 33 and 100 GV/c, at the 95% confidence level.

Cosmic rays provide our only sample of material from outside the solar system. While most cosmic rays probably come from the portion of the galaxy within a thousand light years, it is likely that some fraction has extragalactic origin. For these reasons there have been many searches for cosmic-ray antinuclei.<sup>1-13</sup>

A small flux of antiprotons is expected from cosmic-ray interactions with interstellar material<sup>14, 15</sup> but these reactions should produce negligible fluxes of antihelium and more complex antinuclei. Whereas the observation of antihelium would indicate the presence of cosmologically significant amounts of antimatter, the observation of an antinucleus such as carbon or oxygen would almost certainly imply the existence of antimatter stars capable of nucleosynthesis.

Since matter and antimatter nuclei have opposite signs of charge, they deflect in opposite directions when passing through a magnetic field. We searched for antinuclei by this signature rather than by their characteristic annihilation reactions.

The apparatus (Fig. 1) was a balloon-borne superconducting magnetic spectrometer similar in philosophy to its predecessor.<sup>16</sup> Three sets of optically viewed spark chambers marked the trajectory of each cosmic-ray nucleus as it was deflected by the magnetic field. The view of the

spark chambers in which the greatest deflection occurred was photographed directly by the cameras without the use of mirrors. Four scintillators determined the charge and time of flight for each event; their fourfold coincidence triggered the spark chambers and cameras. A more detailed description of the apparatus is presented elsewhere.<sup>17</sup>

The apparatus was flown from Palestine, Texas, to an altitude of 36 km, leaving a residual 5.4 g/cm<sup>2</sup> of atmosphere above the gondola. The spark locations and digitized scintillator data were photographed for a total of 66 400 triggering events. All photographs were scanned visually for noninteracting single-particle topologies in the spectrometer. Of the 44 909 pictures thus selected, 40 414 were measured automatically on a cathode-ray-tube encoding machine.

We found a sagitta for each event from the direct-view film image by calculating the difference between the measured location of the trajectory at the center spark chamber and the location predicted by a straight line through the measured locations in the outer spark chambers. Because the sagitta was determined solely from direct-view film images, it was directly related to measurement errors. The sagitta was therefore relatively free of potential systematic error because trajectory analysis and a treatment of field integral were unnecessary; however, there was a significant optical distortion due to the spherical aberration of our wide-angle camera lenses. This distortion was calibrated by photographing a grid of regularly spaced points and fitting the measurements with a radial correction. The lens calibration resulted in sagitta corrections averaging 10  $\mu\text{m}$  on the film with a maximum correction of 27  $\mu\text{m}$  and with residuals of about 2  $\mu\text{m}$ .

As a cross check and calibration of our resolution, we turned off the superconducting magnet at the end of the flight so that cosmic-ray nuclei en-

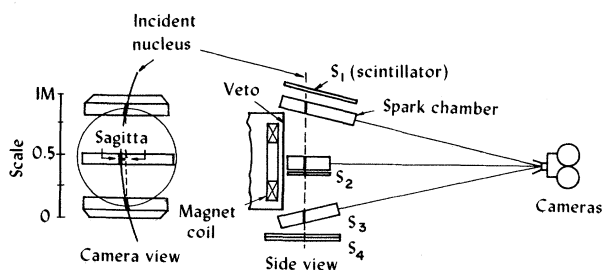


FIG. 1. Schematic drawing of balloon-borne superconducting magnetic spectrometer.

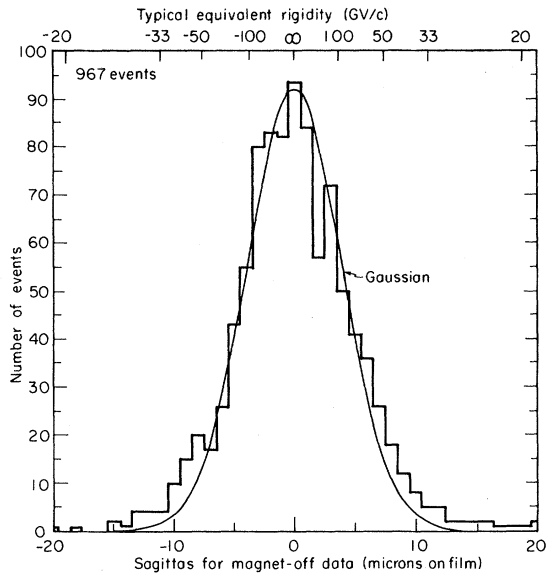


FIG. 2. Histogram of the sagittas of magnet-off events obtained from the manual measurements. Also shown is the Gaussian distribution expected from the combined result of multiple Coulomb scattering and a measurement accuracy of  $3 \mu\text{m}$  on the film (corresponds to  $150 \mu\text{m}$  in the apparatus).

tering our apparatus would pass through undeflected. Figure 2 shows a randomly selected subset of these events as measured on a more accurate manual machine.

Any event whose sagitta had the opposite sign from that of the bulk of the data was listed as an antimatter candidate to be measured on the manual measuring machine. There were two small regions in the apparatus in which the magnetic deflection was small or opposite to the rest of the apparatus. The 2% of the data falling in these two regions were eliminated from consideration. In addition all of the automatically measured events were reconstructed to real space coordinates and then fitted with a legitimate trajectory through the magnetic field. Any event whose reconstructed sparks or fitted trajectory indicated negative deflection was added to the antimatter-candidate list. This selection technique included all events which would have been included by our previous analysis method.<sup>10</sup>

We rejected events whose time-of-flight measurement indicated incidence from below, since high-energy splash albedo nuclei simulate negatively charged nuclei. There were a few hundred such albedo events in the helium data sample, most of which were slow singly charged particles. There were no albedo events of charge  $\geq 3$ .

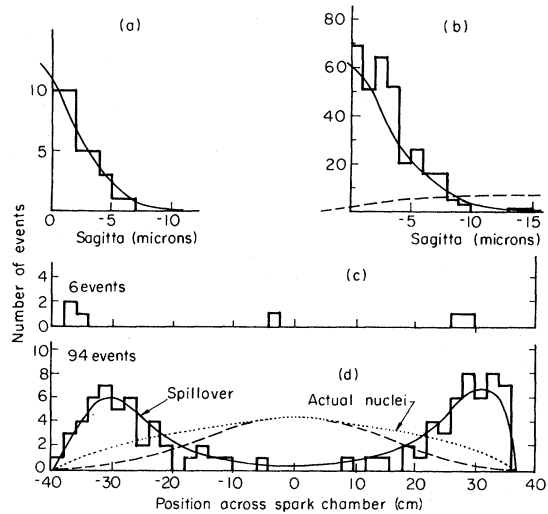


FIG. 3. Histograms of negative-sagitta events showing number versus sagittas for (a) helium and (b) higher-charged nuclei. The dashed curve in (b) represents the expected distribution for an antimatter signal at  $10^{-2}$  of the observed matter signal. The distributions of events with sagittas more negative than  $3.7 \mu\text{m}$  (rigidities less than  $100 \text{ GeV}/c$ ) are also shown as a function of position in the center spark chamber for (c) helium and (d) higher-charged nuclei. In (a), (b), and (d) the solid curves are the expected shapes for nuclei whose sagittas appeared negative as the result of measurement error. For (d) the dotted curve is the distribution of actual nuclei as recorded in the experiment, normalized to the same area as the solid curve. The dashed curve is what an antimatter signal equal to the dotted curve would become after a selection for antimatter candidates; selection efficiency is lower at the sides where the magnetic bending is reduced.

The hand measurements were processed to determine sagittas, and were reconstructed and analyzed to determine each particle's trajectory. Under this more accurate analysis only 546 of the candidates were found to have apparent negative charge.

Nuclear scattering in the center spark chamber or scintillator could have caused a nucleus to have an apparent negative sagitta. For a magnetic field integral of  $5 \text{ kG m}$ , however, the momentum transfer necessary to scatter a nucleus of charge  $Z$  to negative sagitta must be greater than  $100Z \text{ MeV}/c$ . A momentum transfer greater than about  $300 \text{ MeV}/c$  should fragment the incident nucleus. The scattered event would probably have failed our spark-chamber topology requirements or merely given a smaller energy deposition in the bottom scintillators. Six events were rejected for not having a smooth trajectory; these par-

TABLE I. Data summary.

Flight data	Number of nuclei observed per flight		Mean magnetic integral (kG m)
	Helium	Nuclei	
18 Sep 1970 <sup>a</sup>	6131	3152	3.8
7 May 1971 <sup>a</sup>	3838	10 445	4.3
30 Sep 1972	4320	27 630	5.1
Total	14 289	41 227	

Rigidity range (GV/c)	Observed number of antinuclei		Total
	Previous <sup>a</sup>	New	
	Helium		
4 < R < 33	2 ± 3	0	2 ± 3
33 < R < 100	-3 ± 4	≲ 2	-0 ± 5 <sup>c</sup>
	Nuclei Z ≥ 3		
4 < R < 33	0	0	0
33 < R < 100	-8 ± 4 <sup>b</sup>	≲ 4	-0 ± 6 <sup>c</sup>

<sup>a</sup>Previously reported data (Ref. 10).

<sup>b</sup>A minus sign indicates fewer events were observed than were expected from spillover.

<sup>c</sup>In calculating flux limits we took the observed number of events as zero when the previously observed data indicated a negative number and used the errors as representing 68% confidence level.

ticles presumably had scattered in the apparatus. A total of 181 events were rejected for inconsistent scintillator pulse heights; about  $\frac{1}{3}$  of these had the smaller energy deposition.

Figures 3(a) and 3(b) are histograms of the manually measured sagittas for the 35 helium and 324 higher-charged nuclei which remained with apparent negative charge. These events were selected from about 4300 helium and 27 600 higher-charged nuclei. For rigidities (momentum/unit charge) below approximately 33 GV/c our experimental resolution combined with multiple manual measurements provides single-event significance. A rigidity of 33 GV/c corresponded to a sagitta of about 11  $\mu$ m but the sagitta varied depending on the magnetic field integral for the trajectory. For higher rigidities the analysis had to be statistical. As shown in Figs. 3(c) and 3(d), nuclei spilling over to negative sagitta tended to cluster near the edges of the apparatus where the magnetic bending was low, while any true antimatter-signal distribution should have peaked toward the center of the apparatus where the solid-angle acceptance was highest. Our fit to the distribution of candidates across the center spark chamber indicates that for  $Z \geq 3$ , the

TABLE II. Antimatter limits.

Rigidity range (GV/c)	Antimatter-to-matter ratio upper limit (95% confidence)	
	Helium	Nuclei of charge $\geq 3$
4 < R < 33	$5 \times 10^{-4}$	$8 \times 10^{-5}$
33 < R < 100	$2 \times 10^{-2}$	$6 \times 10^{-3}$

number of antimatter nuclei in the rigidity range  $33 < R < 100$  is less than 4 at the 68% confidence level. For the helium nuclei the corresponding number is 2 at the 68% confidence level. An analysis in terms of measured rigidity gave upper limits about 1.2 times larger. Table I is a summary of our present and previous results.

Our efficiency for detecting antimatter candidates was greater than 95% for rigidities between 4 and 33 GV/c, and about 80% for rigidities between 33 and 100 GV/c. Combining the results and taking into account the efficiency, we find the upper limits on the ratio of antimatter to matter fluxes listed in Table II.

To find the corresponding limits in interstellar space these ratios should be increased by 8% for helium and 12% for higher-charged nuclei because of the differential absorption of antimatter and matter in the atmosphere and material of our gondola.

The antimatter flux limits set by our experiments are lower by more than a decade for nuclei of charge  $\geq 3$  and by a factor of 3 for helium than those of previous experiments.

We thank the National Center of Atmospheric Research balloon launch crew at Palestine, Texas, for their hospitality and services.

\*Work supported by Contract No. NAS 9-7801 and Grant No. NGR-05-003-553 from the National Aeronautics and Space Administration and by the Lawrence Berkeley Laboratory.

<sup>1</sup>J. Aizu, Y. H. Fujimoto, S. Hasegawa, M. Koshiba, I. Mito, J. Nishimura, and K. Yokoi, Phys. Rev. **121**, 1206 (1961).

<sup>2</sup>G. Brooks and A. W. Wolfendale, Nature (London) **202**, 480 (1964).

<sup>3</sup>M. V. K. Apparao, Nature (London) **215**, 727 (1967).

<sup>4</sup>N. S. Ivanova, Yu. F. Gagarin, and V. N. Kulikov, Kosm. Issled. **6**, 83 (1968) [Cosmic Res. (U.S.S.R.) **6**, 69 (1968)].

<sup>5</sup>J. G. Greenhill, A. R. Clarke, and H. Elliot, Nature (London) **230**, 170 (1971).

<sup>6</sup>N. L. Grigorov, D. A. Zuravlev, M. A. Kondrat'eva,

I. D. Rapoport, and I. A. Savenko, Zh. Eksp. Teor. Fiz. 45, 394 (1963) [Sov. Phys. JETP 18, 272 (1964)].

<sup>7</sup>E. A. Bogomolov, N. D. Lubyayana, and V. A. Romanov, in *Proceedings of the Twelfth International Conference on Cosmic Rays, Hobart, Australia, 1971*, edited by A. G. Fenton and K. B. Fenton (Univ. of Tasmania, Hobart, Australia, 1972), Vol. 5, p. 1730, Paper No. OG-42.

<sup>8</sup>N. Durgaprasad and P. K. Kunte, Nature (London) Phys. Sci. 234, 74 (1971).

<sup>9</sup>P. Evenson, Astrophys. J. 176, 797 (1972).

<sup>10</sup>A. Buffington, L. H. Smith, G. F. Smoor, L. W. Alvarez, and M. A. Wahlig, Nature (London) 236, 335 (1972).

<sup>11</sup>R. P. Verma, T. N. Rengarajan, S. N. Tandon, S. V. Damle, and Y. Pal, Nature (London), Phys. Sci. 240, 135 (1972).

<sup>12</sup>S. V. Damle, Y. Pal, T. N. Rengarajan, S. N. Tandon, and R. P. Verma, in *Proceedings of the Thirteenth International Conference on Cosmic Rays, Denver, Colorado, 1973* (Univ. of Denver, Denver, Colo., 1973), Vol. 1, p. 231.

<sup>13</sup>R. L. Golden, J. H. Adams, Jr., G. D. Badhwar, C. L. Deney, H. H. Heckman, and P. L. Lindstrom, Astrophys. J. 192, 747 (1974).

<sup>14</sup>T. K. Gaisser and E. H. Levy, Phys. Rev. D 10, 173 (1974).

<sup>15</sup>P. Suh, Astron. Astrophys. 15, 206 (1971).

<sup>16</sup>L. H. Smith, A. Buffington, M. A. Wahlig, and P. Dauber, Rev. Sci. Instrum. 43, 1 (1972).

<sup>17</sup>G. F. Smoot, A. Buffington, C. D. Orth, and L. H. Smith, in *Proceedings of the Thirteenth International Conference on Cosmic Rays, Denver, Colorado, 1973* (Univ. of Denver, Denver, Colo., 1973), Vol. 1, p. 225.

## COMMENTS

### Comment on Large-Momentum-Transfer Photoproduction of $J(3.1)^\dagger$

L. Pilachowski, W. A. Simmons, and S. F. Tuan

*Department of Physics and Astronomy, University of Hawaii at Manoa, Honolulu, Hawaii 96822*

(Received 27 May 1975)

Recent data on photoproduction of  $J^0(3.1)$  suggest that the fraction of events produced with large momentum transfer  $t$  is surprisingly large. Here we comment on a mechanism involving diffractive  $\rho^0$  photoproduction in conjunction with large- $t$   $J^0(3.1)$  production as a possible way of understanding some aspects of the anomaly.

A recent experiment reported by Knapp *et al.*<sup>1</sup> reveals a possibly significant anomaly in the momentum-transfer  $t$  distribution for photoproduction of  $J^0(3.1)$  from a beryllium target at high energy ( $P_{3.1} \geq 80$  GeV/c). Whereas the  $t$  distribution for  $\rho^0$  production from  $\gamma + \text{Be} \rightarrow \rho^0(\rightarrow \pi^+\pi^-) + X$  can be well fitted by

$$\frac{d\sigma}{dt}(\gamma + \text{Be} \rightarrow \rho^0 + X) \sim A^2 e^{40t} + A^{10t}, \quad (1)$$

$$\downarrow \pi^+\pi^-$$

where  $A$  is the Be atomic number and the slopes of the two exponentials,  $\sim 40$  (GeV/c)<sup>-2</sup> and  $\sim 10$  (GeV/c)<sup>-2</sup>, are characteristic respectively of coherent diffractive scattering and incoherent scattering (from single nucleons) of the Be nucleus, the  $t$  distribution of  $J^0(3.1)$  production is in con-

trast of the form

$$\frac{d\sigma}{dt}(\gamma + \text{Be} \rightarrow J^0(3.1) + X) = \beta [A^2 e^{40t} + A e^{bt}], \quad (2)$$

$$\downarrow \mu^+\mu^-$$

where  $b \simeq 4$  (GeV/c)<sup>-2</sup> is consistent with the preliminary data<sup>1</sup> [indeed a smaller value  $b \simeq 1.5$  to 2 (GeV/c)<sup>-2</sup> from increased data has been suggested] and  $\beta$  is a normalization constant. Hence though  $J^0(3.1)$  shares the same common feature with the  $\rho^0$  of being diffractively photoproduced (narrow forward peak from  $e^{40t}$  term), it differentiates also sharply from the  $\rho$  meson in that a copious fraction of 3.1 events are produced with large momentum transfer  $t$  [ $b \ll 10$  in second exponentials of Reactions (1) and (2)]. There are indications<sup>2</sup> that this feature ( $b \ll 10$ ) may also be present at the lower Stanford Linear Accelerator Center photon energy ( $\sim 20$  GeV) for  $\gamma + p \rightarrow J^0 + X$ .